JIPB Journal of Integrative Plant Biology

Transcript profiling of a novel plant meristem, the monocot cambium[FA]

Matthew Zinkgraf[1,2], Suzanne Gerttula[1] and Andrew Groover[1,3]*

1. US Forest Service, Pacific Southwest Research Station, Davis, California, USA
2. Department of Computer Science, University of California, Davis, USA
3. Department of Plant Biology, University of California, Davis, USA
*Correspondence: Andrew Groover (agroover@fs.fed.us)
doi: 10.1111/jipb.12538

Research Article

Abstract While monocots lack the ability to produce a vascular cambium or woody growth, some monocot lineages evolved a novel lateral meristem, the monocot cambium, which supports secondary radial growth of stems. In contrast to the vascular cambium found in woody angiosperm and gymnosperm species, the monocot cambium produces secondary vascular bundles, which have an amphivasal organization of tracheids encircling a central strand of phloem. Currently there is no information concerning the molecular genetic basis of the development or evolution of the monocot cambium. Here we report high-quality transcriptomes for monocot cambium and early derivative tissues in two monocot genera, *Yucca* and *Cordyline*. Monocot cambium transcript profiles were compared to those of vascular cambia and secondary xylem tissues of two forest tree species, *Populus trichocarpa* and *Eucalyptus grandis*. Monocot cambium transcript levels showed that there are extensive overlaps between the regulation of monocot cambia and vascular cambia. Candidate regulatory genes that vary between the monocot and vascular cambia were also identified, and included members of the KANADI and CLE families involved in polarity and cell-cell signaling, respectively. We suggest that the monocot cambium may have evolved in part through reactivation of genetic mechanisms involved in vascular cambium regulation.

Edited by: Chun-Ming Liu, Institute of Crop Science, CAAS, China
Received Feb. 18, 2017; **Accepted** Mar. 15, 2017; **Online on** Mar. 17, 2017
FA: Free Access, paid by JIPB

Free Access

INTRODUCTION

The vascular cambium is a lateral meristem found in diverse angiosperm and gymnosperm species, and is responsible for supporting the radial, woody growth of stems. The vascular cambium consists of meristematic initials that divide over time to produce daughter cells which in turn divide before differentiating into cell types of secondary xylem (wood) toward the inside of the stem, or secondary phloem (inner bark) toward the outside of the stem. During angiosperm evolution, monocots lost the ability to produce a vascular cambium and thus do not produce secondary xylem or secondary phloem.

The loss of vascular cambium in monocots may have resulted from differences in the anatomy of primary vascular bundles in stems of monocots versus other angiosperm lineages capable of secondary growth. In angiosperms such as a poplar tree that possess a vascular cambium, primary vascular bundles are typically arranged in a ring around the periphery of the stem, and have an open collateral anatomy with xylem toward the inside and phloem toward the outside of the bundle (Esau 1977). In many species, a fascicular vascular cambium can form between the primary phloem and xylem, and subsequent cell divisions by the fascicular cambium create files of cells consisting of secondary xylem and secondary phloem. In species with more extensive secondary growth, interfascicular cambium forms and joins with fascicular cambia to create a single, continuous cambium layer. In monocots, vascular bundles are scattered throughout the stem, precluding the coordinated production of a single ring of meristematic tissue through an analogous process.

But perhaps more importantly, all cells within monocot vascular bundles ultimately differentiate and the bundles are closed, being surrounded by a layer of terminally differentiated schlerenchyma cells.

In some monocot lineages, radial growth of stems is achieved through the action of a lateral meristem termed the monocot cambium. The monocot cambium, also referred to as the secondary thickening meristem and other terms in the literature (Jura-Morawiec et al. 2015), has been the subject of several studies aimed at describing the underlying anatomy and morphogenesis, which have been summarized in recent reviews (Carlquist 2012; Jura-Morawiec et al. 2015). Those species possessing a monocot cambium have been described (Rudall 1995), and are distributed within the Asparagales, including species within genera *Yucca* and *Cordyline* used in experiments here. Some species within Asparagales lack a monocot cambium, leading to the assumption that this meristem has arisen multiple times, or has been lost multiple times within this lineage (Rudall 1995). While variation among species must be acknowledged, the monocot cambium is a meristematic layer in the stem that undergoes periclinal divisions to produce foci of meristematic cells toward the center of the stem, which in turn differentiate into secondary vascular bundles (Cheadle 1937; Tomlinson and Zimmermann 1967, 1969; Diggle and DeMason 1983a, 1983b; Rudall 1991). Mature secondary bundles have an amphivasal organization, with xylem surrounding a core of phloem. Toward the outside of the stem, the monocot cambium produces a modest amount of secondary cortex.

A number of interesting evolutionary and developmental biology questions are presented by the monocot cambium. The ancestral state of angiosperms was likely characterized by a vascular cambium and woody growth (Spicer and Groover 2010), with the vascular cambium and secondary xylem lost in monocots. Thus, the evolution of this novel monocot cambium meristem and associated developmental processes provides the opportunity to address questions fundamental to how genes and mechanisms evolve to produce novel structures and development in plants. For example, did the monocot cambium arise *de novo*, or were genes or mechanisms regulating the vascular cambium or another meristem co-opted during the evolution of this new meristem? It is also not known if mechanisms described for patterning and polarity of primary vascular bundles in Arabidopsis (Emery et al. 2003; Ilegems et al. 2010) might be involved in producing the amphivasal organization of the monocot secondary vascular bundles, or how the longitudinal continuity of secondary vascular bundles is coordinated during development. Genes affecting the initiation, maintenance and patterning of tissues derived from the vascular cambium have been identified, making these tractable questions. For example, in poplar Class I KNOX transcription factors ARBORKNOX1 and 2 have been described that affect both cambium function and the regulation of differentiation of cambial daughter cells (Groover et al. 2006; Du et al. 2009); the Class III HD ZIP transcription factor popREVOLUTA affects patterning of secondary vascular tissues (Robischon et al. 2011), and the balance of division and differentiation is affected by CLAVATA3 (CLV3)/EMBRYO SURROUNDING REGION (ESR)-RELATED (CLE) WUSCHEL- signaling from the phloem across the cambial zone (Etchells et al. 2015).

In the studies here, we describe gene transcript profiles for monocot cambium and derived tissues from two genera, *Yucca* and *Cordyline*. High quality transcriptomes are described, and the global functions of expressed genes are contrasted with transcript profiles from wood-forming tissues of model angiosperm trees (*Populus* and *Eucalyptus*). Our results provide evidence supporting the hypothesis that significant co-option of genes and mechanisms regulating vascular cambia were involved in the evolution of monocot cambia.

RESULTS

Anatomy and sampling of monocot cambia

Healthy, actively growing specimens of two species with a monocot cambium, *Cordyline australis* and *Yucca gloriosa*, were destructively harvested for histology and gene transcript profiling experiments (Materials and Methods). As shown in Figure 1 for a *Cordyline australis* specimen, each plant's stem was cut at the ground level and below the foliage. The inner anatomy of the stem is shown in Figure 1B, with the central portion of the stem produced by primary growth of the apical meristem and primary thickening meristem, surrounded by a cylinder of secondary tissues produced by radial growth of the monocot cambium. The outermost portion of the stem is composed of tightly appressed leaf bases. A vertical incision in these actively growing stems allowed the secondary tissues to be separated at the monocot

Figure 1. Tissues harvested
(**A**) Plants sampled for histology and sequencing included a 9-year-old *Cordyline australis* grown in an irrigated garden in Woodland, California. (**B**) A cross-section from the same plant, showing tissues produced during primary growth from the apical and primary thickening meristems (1°) and tissues produced by secondary growth from the monocot cambium (2°). (**C**) Stems were peeled, separating at the monocot cambium layer, and cells harvested from both the secondary cortex (SC) layer produced by the outer face of the monocot cambium and the inner layer containing secondary vascular bundles (SVB) produced by the inner face of the monocot cambium.

cambium layer (Figure 1C). Samples for transcript profiling were harvested by lightly scraping both the inner and outer faces of the separated tissues to capture both the monocot cambium and recent derivatives.

The anatomy of a *Cordyline* stem sampled for transcript profiling is summarized in Figure 2. The inner face of the monocot cambium produces extensive growth composed of individual secondary vascular bundles within a background of unlignified cells (Figure 2A). The outer face produces less growth, composed of secondary cortex transversed by leaf vascular traces (Figure 2B). The monocot cambial zone can be detected by virtue of the cell files produced by transverse divisions (Figure 2C). Secondary vascular bundles are first seen as small groups of dividing cells produced by the monocot cambium that differentiate beginning at the leading edge of cells first produced by the monocot cambium, followed by progressive differentiation toward the trailing edge of cells (Figure 2C). Mature bundles have an amphivasal organization, with xylem surrounding phloem (Figure 2D). Remarkably, the development of secondary vascular bundles is coordinated axially to produce long bundles (Figure 2E, F). The anatomy of a *Yucca* stem sampled for transcript sequencing is summarized in Figure 3. The overall organization is similar to that seen for *Cordyline*, except the proportion of vascular bundles is lower relative to the background of unlignified

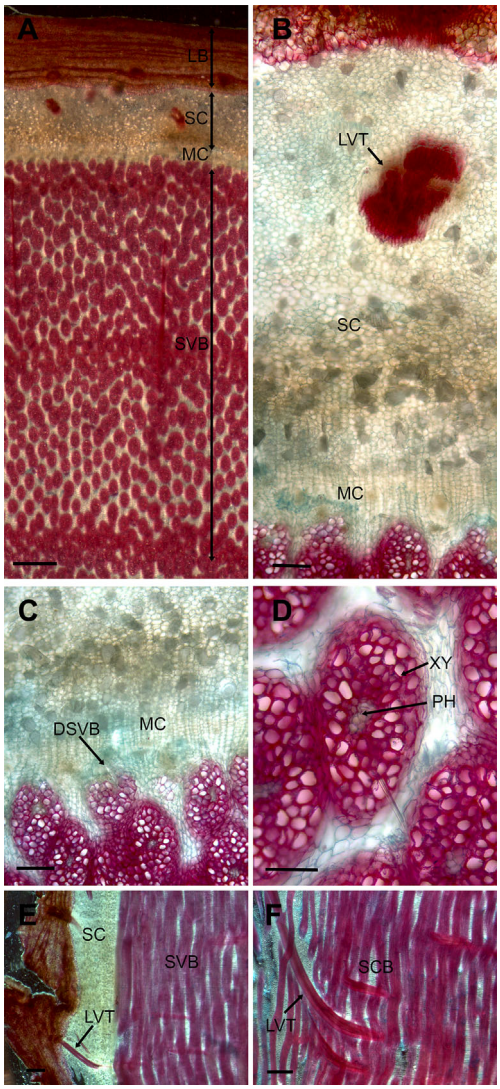

Figure 2. *Cordyline* anatomy
(**A**) Transverse section of *Cordyline* stained with phloroglucinol to reveal lignified cells (red color). The inner face of the monocot cambium (MC) layer produced secondary vascular bundles (SVB), while the outer face produced secondary cortex (SC). The outer layer of the stem is unsheathed with leaf bases (LB). (**B**) Cell files can be seen associated with the periclinal divisions of the monocot cambium (MC). Leaf vein traces (LVT) traverse the secondary cortex. (**C**) Developing secondary vascular bundles (DSVB) appear first as foci of dividing cells, and differentiate from the inner to outer portion of the bundle. (**D**) Mature secondary vascular bundles have an amphivasal arrangement of xylem (XY) surrounding phloem (PH). (**E**, **F**) Anastomosing secondary vascular bundles can be seen in longitudinal sections, which can be traversed by leaf vein traces. DSVB, developing secondary vascular bundle; LB, leaf base; LVT, leaf vein trace; MC, monocot cambium; PH, phloem; SVB, secondary vascular bundle; XY, xylem. Scale bars: A = 2 mm, B–D = 200 μm, E = 2 mm, F = 1 mm.

cells, and the differentiation of secondary vascular bundles is more graded (Figure 3A, B).

De novo assembly of transcriptomes

Illumina sequencing libraries were prepared for each sample (Materials and Methods) and sequenced as 100 base pair, paired end reads. Sequencing statistics are presented in Table 1, and after processing the sequencing reads (Materials and Methods) over 169 M high-quality reads were produced for the two monocot species surveyed. *De novo* assembly of transcriptomes for the two species was performed using the Trinity package, and resulting transcript scaffolds were further processed

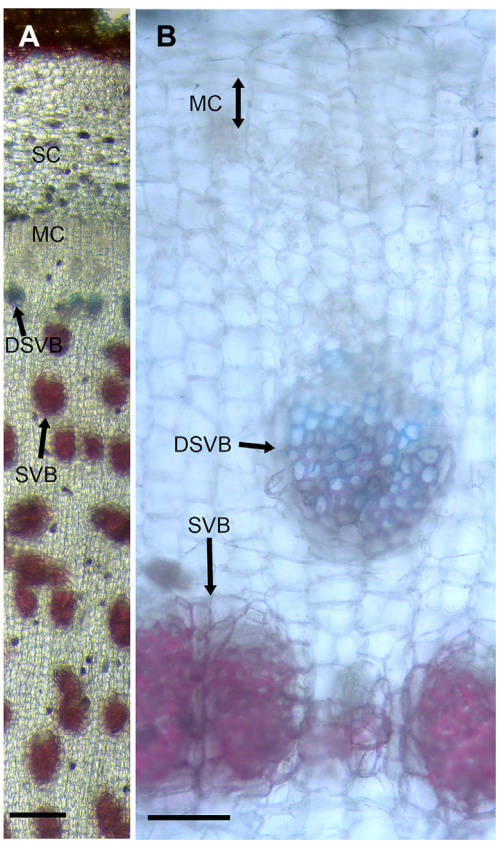

Figure 3. *Yucca* anatomy
(**A**) Transverse section of *Yucca* stained with phloroglucinol. This *Yucca* specimen produced a lower density of secondary vascular bundles when compared with *Cordyline*. (**B**) Cell files associated with periclinal divisions of the monocot cambium (MC) are indicated. Developing secondary vascular bundles develop in a graded manner, beginning with the portion toward the center of the stem. DSVB, developing secondary vascular bundle; MC, monocot cambium; SC, secondary cortex; SVB, secondary vascular bundle. Scale bars: A = 2mm, B = 200 μm.

and filtered based on quality, redundancy and coding potential using the tr2aacds pipeline from EvidentialGene (http://arthropods.eugenes.org/EvidentialGene/evigene/). A total of 33,195 and 26,651 scaffolds were produced for *Yucca* and *Cordyline*, respectively. Quality measures of the scaffolds are presented in Table 2. Sequencing reads were mapped to these scaffolds to quantify transcript levels associated with each scaffold. Orthologous relationships among monocot scaffolds and genes from poplar and eucalyptus were determined using InParanoid (Sonnhammer and Östlund 2015), and annotations were taken from the best BLAST match from *Arabidopsis* (Materials and Methods).

Monocot and vascular cambia express similar biological processes

Using the transcript scaffolds as a representation of expressed genes, gene expression in the monocot cambium samples was compared to genes expressed in the cambium and wood-forming tissues for two forest tree species, *Populus* and *Eucalyptus*. Transcript levels within species and comparisons of ortholgous transcripts among species is detailed in Table S1. As summarized in Figure 4 and detailed in Table S2, Gene Ontology (GO) terms were compared for the transcriptomes of the two monocot species to genes expressed in *Populus* and *Eucalyptus* (Materials and Methods) and revealed a surprising degree of overlapping processes, with 5,345 of a total of 6,527 GO terms shared among all four species. Only 127 GO terms were uniquely associated with the two monocot species and not shared by *Populus* or *Eucalyptus* (Figure 4).

KNOX genes are expressed in both monocot and vascular cambia

KNOX transcription factors are evolutionarily ancient (Hay and Tsiantis 2010), and include major regulators of both shoot apical meristems and vascular cambia. For example, previous studies showed poplar Class I KNOX genes *ARBORKNOX1* (*ARK1*) and *ARK2* (orthologous to *Arabidopsis SHOOTMERISTEMLESS* and *BREVIPEDICELLUS/KNAT1*, respectively) play critical roles in the vascular cambium function and cell differentiation during wood formation (Groover et al. 2006; Du et al. 2009), while Class II KNOX transcription factor KNAT7 regulates cell wall biosynthesis in both *Arabidopsis* and *Populus* (Li et al. 2012). Transcript abundance was quantified for KNOX gene orthologs from wood-forming tissues of *Populus* and *Eucalyptus*, and for monocot cambium samples, and are presented as heatmaps of transcript levels for each species in Figure 5. For each of five KNOX genes, expressed scaffold orthologs were identified from the monocot cambium tissues. Thus, the monocot cambia share the quality of KNOX gene regulation with vascular cambia.

Polarity and patterning-related gene expression

Class III HD ZIP transcription factors act antagonistically with KANADI GARP transcription factors in establishing auxin-dependent patterning and polarity during embryogenesis and vascular development in *Arabidopsis* (Izhaki and Bowman 2007; Ilegems et al. 2010). Class III HD ZIPs have been shown to also play roles in regulating differentiation, cambium initiation and tissue polarity during secondary growth in *Populus* (Du et al. 2011; Robischon et al. 2011). Interestingly, misregulation of key Class III HD ZIPs or KANADIs can result in vascular bundles with an amphivasal pattern with xylem surrounding phloem (Emery et al. 2003), as is seen in the secondary vascular bundles produced by the monocot cambia.

As shown in Figure 6A, expressed monocot transcript scaffolds were identified for each of the clades of Class III HD ZIPs. However, there was variation between *Yucca* and *Cordyline*, and only *Yucca* scaffolds were found for REVOLUTA and PHABULOSA/PHAVOLUTA-like genes. Because of limitations of our sampling

Table 1. Quality statistics for RNA sequencing data used in transcriptome assemblies

Species	Dataset	# Raw reads	# Quality reads[a]
Yucca	Pooled_seq_1	179,199,988	98,746,242
Cordyline	Pooled_seq_1	165,829,174	84,275,326
	Pooled_seq_2	171,368,754	94,917,520
	Total	337,197,928	179,192,846

[a]The total number of reads that had a quality threshold greater than 30 and read length greater than 36 bp after trimming.

Table 2. Transcriptome assembly statistics

Species	Assembly method		Number scaffolds	Length (nt)	N50	GC (%)	Mapping (%)
Yucca	trinity *de novo*		104,396	111,875,370	1,417	43.05	97.79
	trinity *de novo*	tr2aacds	33,195	40,601,780	1,576	45.52	96.01
Cordyline	trinity *de novo*		92,165	106,072,491	1,589	41.43	98.56
	trinity *de novo*	tr2aacds	26,651	35,510,388	1,768	44.17	88.30

The percentage of quality reads that mapped to the assembly was determined using bowtie2 and the Trinity utility SAM_nameSorted_to_uniq_count_stats.pl

and lack of genome sequence references for these species, it is not possible to determine if this result could reflect gene loss in the *Cordyline*, or differences in growth and development between *Cordyline* and *Yucca* (see Discussion). No evidence was found for mutations in the binding site for the micro RNAs (miRNAs) that negatively regulate Class III HD ZIP transcripts for monocot scaffolds containing that region (data not shown).

More strikingly, *KANADI*-like genes showed a strong difference in expression between the monocot species and tree species. As shown in Figure 6B, both *Cordyline* and *Yucca* showed expression of multiple *KANADI*-like genes, while no expression was found in the cambium and wood-forming samples from *Populus* and *Eucalyptus*. There are at least two confounded interpretations of this result. First, although *KANADI* gene expression patterns have not been specifically studied in trees, their characteristically abaxial expression in herbaceous organs would suggest that their expression would be in the secondary phloem in the tree species. Consistent with that expectation, comparison of RNAseq transcript levels from wood versus bark scraping in two poplar species shows that *KANADI*-like genes show preferential expression in bark (Figure S1). The *KANADI*-like transcripts in the monocot samples could come from cells scraped from abaxial cortical tissues produced by the monocot cambium, from the phloem cells found within the secondary bundles, or could reflect some other expression that is fundamentally different from the vascular cambia.

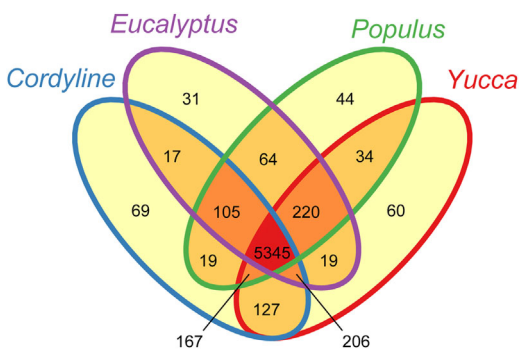

Figure 4. Venn diagram indicating the overlap of Gene Ontology terms for expressed genes in all possible comparisons among the four species

Genes involved in CLE-WOX signaling evidence for both conserved and derived functions

Signaling circuits have been described in which secreted peptides encoded by the CLAVATA3 (CLV3)/EMBRYO SURROUNDING REGION (ESR)-RELATED (CLE) gene family interact with LEUCINE-RICH REPEAT RECEPTOR-LIKE KINASEs (LRR-RLKs), and can affect developmental processes through mechanisms including modulation of WUSCHEL-related HOMEOBOX (WOX) transcription factors and hormone-related mechanisms (Kondo and Fukuda 2015). Most relevant to the monocot cambium, CLE-WOX signaling has been implicated in *Arabidopsis* in the regulation of xylem cell differentiation (Ito et al. 2006) and in the regulation of the vascular cambium through secretion of the phloem-expressed CLE41/TRACHEARY ELEMENT DIFFERENTIATION FACTOR (TDIF), which is perceived by the cambial-expressed TDIF RECEPTOR/ PHLOEM INTERCALATED WITH XYLEM (PXY) LRR-RLK. This signaling in turn modulates the expression of *WOX4*, a transcriptional regulator of cambial cell proliferation (Etchells and Turner 2010; Hirakawa et al. 2010). This same signaling circuit has also been shown to function in cambial regulation in poplars (Etchells et al. 2015).

As shown in Figure 7A, expression of different CLE family members varies among the tissue samples for all four species. Some of this variation could likely reflect differences in anatomy and sampling, for example with different amounts of cambium and secondary phloem within xylem scrapings from *Populus* and *Eucalyptus*

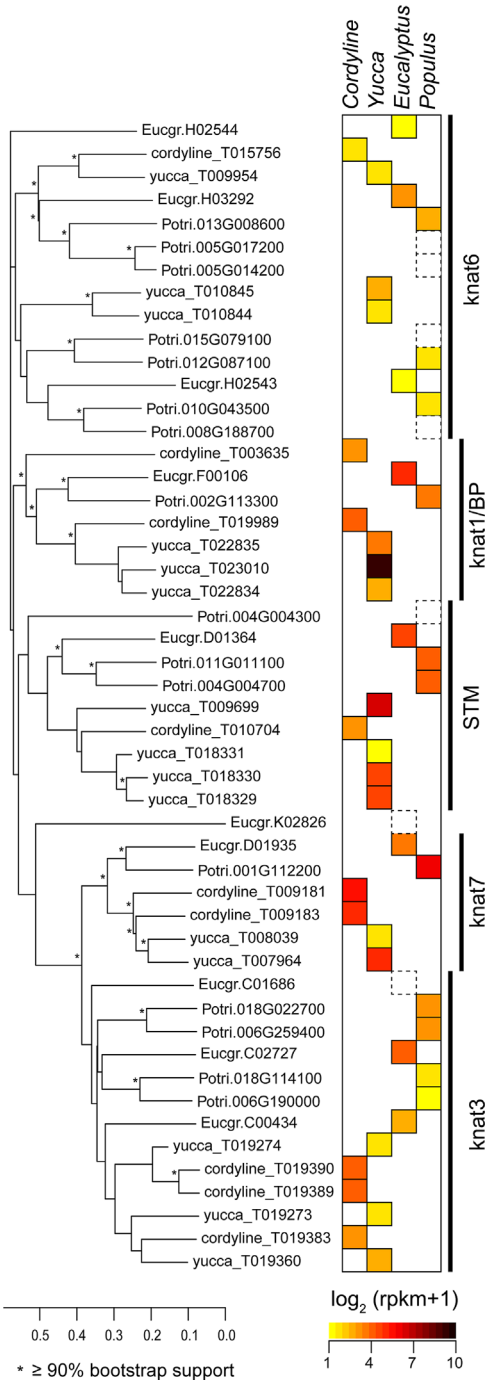

Figure 5. Comparison of transcript levels for KNOX transcription factor-encoding genes among the four study species

Phylogenetic trees were established among annotated genes from *Populus* and *Eucalyptus* and transcript scaffolds from *Cordyline* and *Yucca*. Asterisks indicate bootstrap values of > 0.9. Transcript levels were estimated as $\log_2$ (reads per kilobase per million reads (rpkm) $+ 1$) and shown in heat map intensity (see scale in legend). Dashed boxes indicated genes or scaffolds with expression below the 1 rpkm threshold.

(see Discussion). However, only two CLE family members showed any expression within a monocot cambia sample. This could reflect inherently low expression or localized expression, resulting in inability to detect other family members, or could reflect a particular biological feature of the monocot cambium. For potential downstream *WOX* genes (Figure 7B), vascular cambium-expressed WOX4-like genes were expressed in both tree species and in *Yucca*. A *WOX4*-like *Cordyline* scaffold was assembled but had read count numbers below our cutoff for calling expression. Conversely, a *WOX11*-like scaffold showed significant expression while none of the other three species expressed *WOX11*-like orthologs. All four species had expression of *WOX13*-like genes, and *PXY*-like gene expression was also found in all four species samples (Figure 7C).

DISCUSSION

Our results overall show considerable overlap of gene expression and associated mechanisms between monocot cambia and derivatives of *Yucca* and *Codyline* species and vascular cambia and developing secondary xylem of two forest trees (*Populus* and *Eucalyptus* species). For example, over 80% of GO terms taken from expressed genes were shared by monocot and vascular cambia samples, and key regulators of vascular cambia including Class I KNOX and Class III HD ZIP transcription factor-encoding genes were also expressed in monocot cambia samples. Because vascular cambium and wood formation are ancestral traits that were lost in monocot lineages, the most parsimonious interpretation of these results would be that key genes and mechanisms that regulate vascular cambia were co-opted and reactivated in the evolution of monocot cambia. However, this interpretation does not explain the obvious anatomical differences between the tissues produced by monocot versus vascular cambia, including the amphivasal secondary vascular bundles with xylem surrounding phloem produced by the monocot cambia.

The unique anatomy of the monocot cambia sampled present interesting questions and additional complications in interpreting our gene expression data. Our forest tree samples would be expected to include small proportions of cells from the cambial zone, in addition to developing secondary xylem and rays. Our monocot

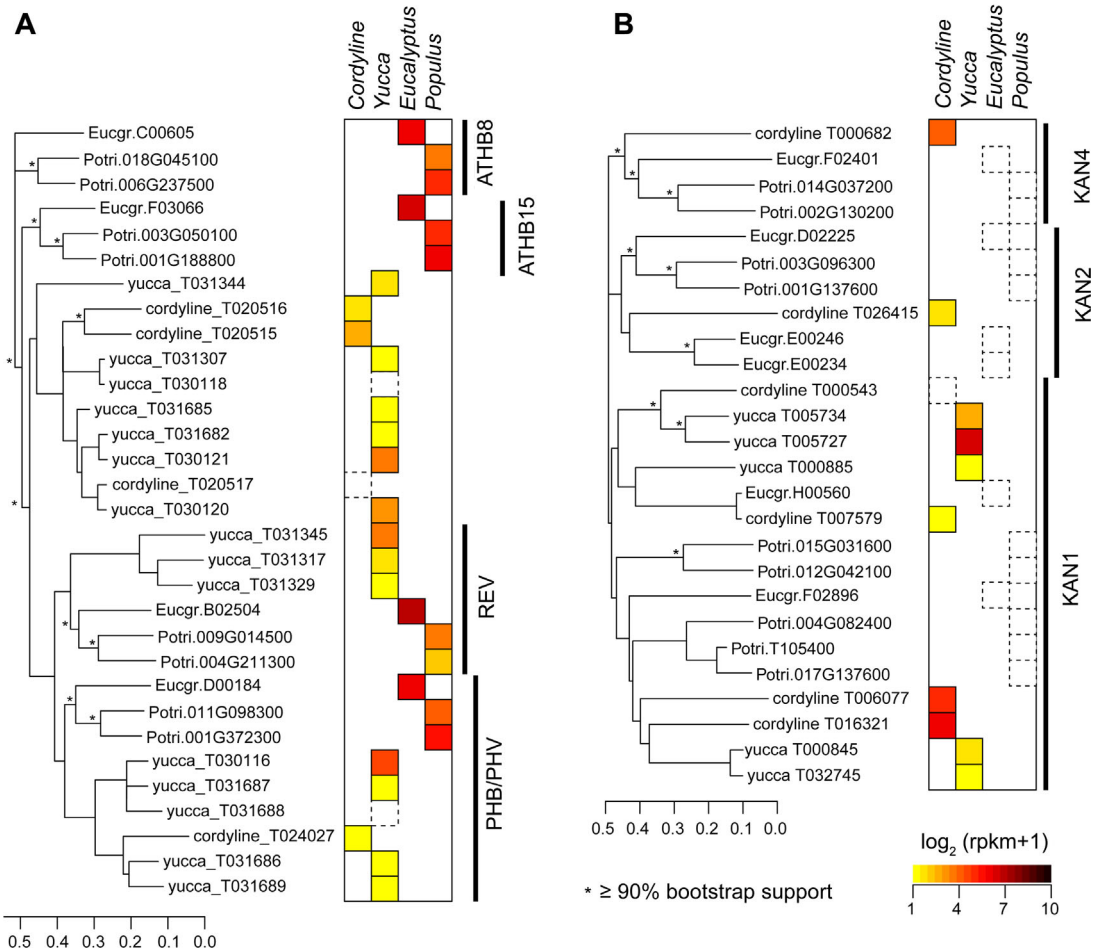

Figure 6. Comparison of transcript levels for (A) Class III HD ZIP and (B) KANADI encoding genes among the four study species

Phylogenetic trees were established among annotated genes from *Populus* and *Eucalyptus* and transcript scaffolds from *Cordyline* and *Yucca*. Asterisks indicate bootstrap values of > 0.9. Transcript levels were estimated as $\log_2$ (reads per kilobase per million reads (rpkm)+1) and shown in heat map intensity (see scale in legend). Dashed boxes indicated genes or scaffolds with expression below the 1 rpkm threshold.

cambium samples contained the monocot cambium, a small amount of cortex produced toward the outer face of the cambial layer, and the secondary bundles and associated parenchyma produced by the inner face of the cambial layer. Notably, each secondary vascular bundle has an amphivasal arrangement of xylem surrounding phloem: thus our monocot samples contained phloem tissues, while the tree samples did not. We examined genes associated with polarity of vascular tissues, including *Class III HD ZIPs* and *KANADI* genes, the misregulation of which can produce amphivasal bundles in *Arabidopsis* (Emery et al. 2003). We found no evidence for significant expression differences for *Class III HD ZIPs* when comparing monocot and vascular cambia samples, but did see that *KANADI*-like genes were expressed in monocot cambial but not vascular cambial samples. Class III HD ZIPs have been previously shown to be adaxially/xylem-expressed in both *Arabidopsis* (Emery et al. 2003; Prigge et al. 2005) and poplar trees (Du et al. 2011; Robischon et al. 2011). *KANADIs* have not been functionally characterized in trees, but the abaxial expression of *KANADI1* in *Arabidopsis* (Kerstetter et al. 2001; Eshed et al. 2004) would raise the expectation that, if they are expressed during angiosperm secondary growth, *KANADI*-like genes would likely be expressed in the abaxial secondary phloem (which was not sampled here). The expression of *KANADI*-like genes in the monocot cambium samples could simply reflect the presence of

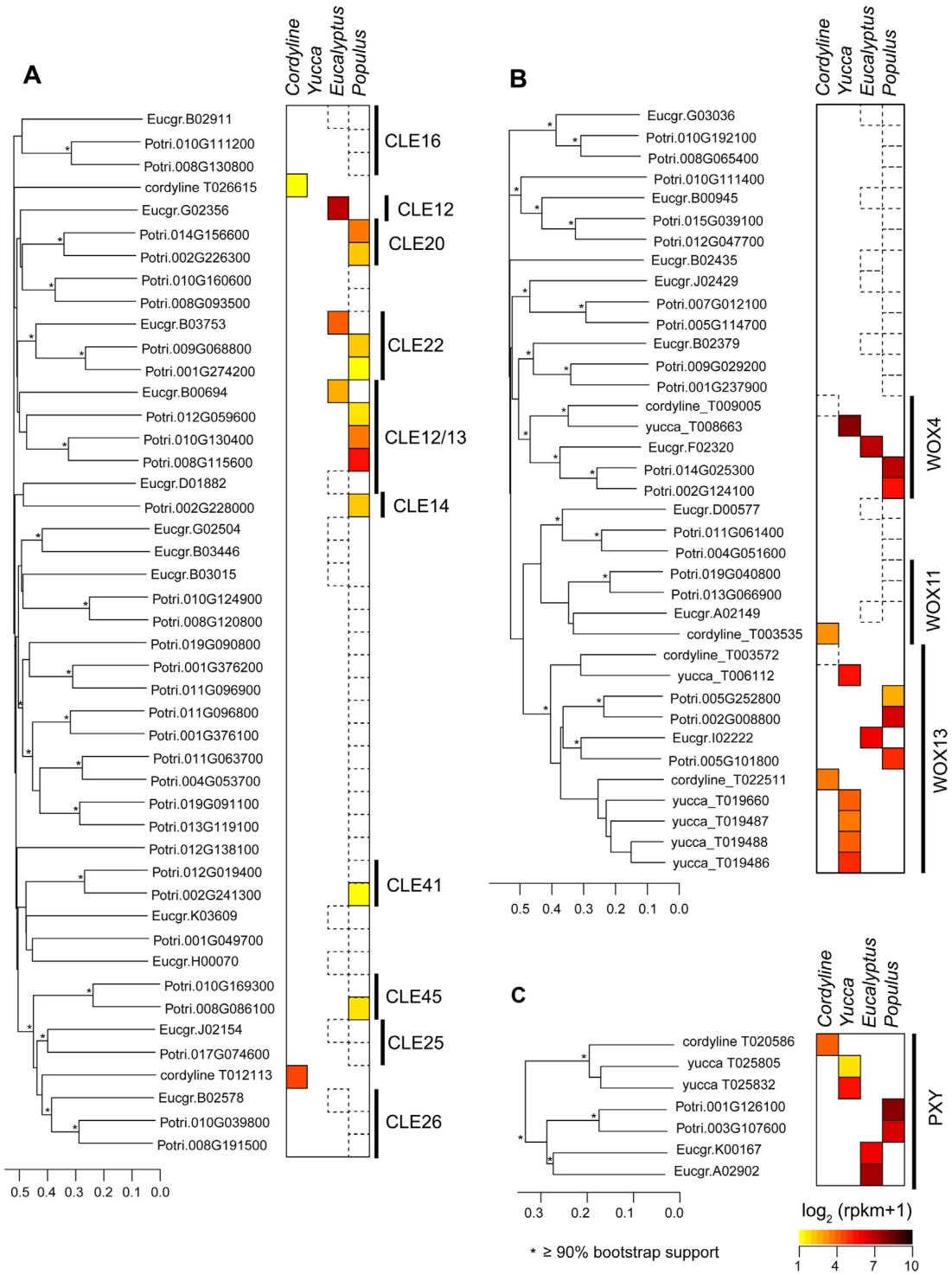

Figure 7. Comparison of transcript levels for (A) CLE-like peptide encoding genes (B) WUSCHEL-related HOMEOBOX (WOX) transcription factor encoding genes, and (C) PHLOEM INTERCALATED WITH XYLEM (PXY)-like LEUCINE-RICH REPEAT RECEPTOR (LRR) encoding genes among the four study species

Phylogenetic trees were established among annotated genes from *Populus* and *Eucalyptus* and transcript scaffolds from *Cordyline* and *Yucca*. Asterisks indicate bootstrap values of > 0.9. Transcript levels were estimated as $\log_2$ (reads per kilobase per million reads (rpkm) $+ 1$) and shown in heat map intensity (see scale in legend). Dashed boxes indicated genes or scaffolds with expression below the 1 rpkm threshold.

phloem within the tissues sampled (secondary vascular bundles). Alternatively, it could indicate a causative role for *KANADI*-like genes in producing the striking amphivasal arrangement of the secondary vascular bundles. Likewise, variation in expression of *CLE*-like genes between vascular and monocot cambium samples could be a reflection of anatomical differences, or could indicate a causative role of CLE-like genes in generating patterning differences of tissue derived from the two meristems.

Some important factors must be considered when further interpreting our gene expression results and seeking candidate genes responsible for the unique anatomy produced by the monocot cambia. First, there are no reference genomes for the *Yucca* and *Cordyline* species studied, and we are limited to examining genes that were expressed in the tissues sampled and cannot discriminate between the presence or absence of a gene in these monocot lineages versus lack of expression. Similarly, we cannot determine if differences seen in gene expression between the two monocot species sampled reflect true species differences in gene content, or differences in gene expression associated with growth and development. While overall anatomy is similar, we did note variation between the *Cordyline* and *Yucca* plants sampled, with the *Yucca* showing a lower density of secondary vascular bundles. Indeed, it is not clear from previous surveys of other species within the Asparagales (Rudall 1995) if the monocot cambium in *Yucca* and *Cordyline* were present in their last common ancestor, or if they independently acquired a monocot cambium. Further investigation will be required to determine the significance of differences seen in gene expression between our *Cordyline* and *Yucca* samples, including addressing whether the monocot cambia in these lineages arose independently or share a common ancestral origin.

Future studies will be required to fully understand the evolution and development of the monocot cambium. A reference genome for at least one species possessing a monocot cambium would be extremely helpful in interpreting gene expression data with regard to potential gene loss versus lack of expression. The size of the stems would be a significant technical challenge, but *in situ* hybridization, laser capture microscopy, or some other technique that would be capable of determining the spatial expression of regulatory genes within the monocot cambium and derived secondary tissues would be extremely helpful in interpreting gene expression data from tissue samples containing multiple tissues and cell types. Additionally, it would be helpful to have more information about the genes and mechanisms responsible for the differences in the distribution and development of primary vascular bundles in monocots versus dicots. Is it possible that the secondary vascular bundles differentiate as a default from meristematic tissues using the same mechanisms as primary bundles? If so, explaining the rest of the mechanisms controlling the initiation and maintenance of the monocot cambium might suffice to provide an overall view of the development of this unusual set of plant tissues.

MATERIALS AND METHODS

Plants and tissue sample processing

Three plants were used in the experiments here: (i) a *Cordyline australis* 4.3 m tall and 9 years old was harvested from an irrigated home garden in Woodland, California; (ii) a *Cordyline australis*, cv "Torbay Dazzler" 0.4 m tall and 3 years old was harvested from a greenhouse in Placerville, California; and (iii) a *Yucca gloriosa* 0.5 m tall and 3 years old was harvested from the same greenhouse. All plants were actively growing and healthy at the time of harvest in September of 2012.

Tissue was harvested by cutting stems into sections, and then making a vertical incision through the leaf bases ensheathing the stem. Leaf bases were then peeled back, cutting the leaf traces to release the underlying stem. The exposed tissues on both sides of the stem were then scraped with a double-edged razor blade to harvest the monocot cambium layer and recent derivatives, including developing secondary vascular bundles. Tissues were immediately frozen in liquid nitrogen and stored at 80 °C prior to RNA isolation.

Total RNA was isolated using a multi-step process. First, each tissue sample was ground using a mortar and pestle chilled with liquid nitrogen, and then extracted using TRIzol Reagent (Invitrogen, Carlsbad, CA, USAL) following the manufacturer's protocol for plant tissues. Second, each sample was treated with RNAse-free DNAse in 1 RDD buffer (Qiagen 79254; Qiagen,

Valencia, CA, USA) at 37° for 45 min. Third, the DNAsed RNA was purified using the Qiagen Plant RNA Mini kit (Qiagen 74903) following the manufacturer protocol, and eluting with 60 uL of RNAse-free water. Each RNA sample was determined to be high quality using both a Qubit (ThermoFisher, Waltham, MA, USA) fluorimeter to assay quantity, and a Bioanalyzer (Agilent, Santa Clara, CA, USA) to assay quantity and quality.

Libraries for sequencing were prepared using the Illumina TruSeq mRNA Sample Prep kit V2 (Illumina, San Diego, CA, USA) following the manufacturer's protocol. Samples were subjected to Illumina HiSeq 100 base pair paired-end sequencing at the QB3 Vincent J. Coates Genomics Sequencing Laboratory (University of California, Berkeley, CA, USA) in January of 2013.

Histology

Stem pieces were pickled by placing them in 25% reagent grade alcohol for 2 d, then in 50% reagent grade alcohol for 2 weeks with regular changes to fresh solution. Stem pieces were further dissected to make blocks containing the monocot cambium and recent derivatives, and sectioned using a sliding microtome. Sections were stained using phloroglucinol. Images were captured using a Leica DM compound microscope with a digital camera and Live Image Builder software (Leica) for creating larger format images.

Bioinformatics

The transcriptomic data from the four species analyzed in this study were uniformly processed using the following steps. First, RNA-seq datasets for developing xylem from *Populus* (*P.* euramericana) and *Eucalyptus* (*E. grandis*) were downloaded from the National Center for Biotechnology Information (NCBI) short reads archive in October 2016 (PRJNA223526; Xu et al. 2014). Second, potential adaptor contamination was identified and removed from the raw fastq reads using scythe v0.950 (https://github.com/vsbuffalo/scythe). Third, reads were trimmed based on a quality threshold of 30 and reads were kept if the minimum length after trimming was greater than 36 bp using sickle v1.200 in paired-end mode (Joshi and Fass 2011) (https://github.com/najoshi/sickle).

De novo transcriptome assemblies for each monocot species were generated using a two-step approach to produce high-quality non-redundant assemblies. First, processed Illumina reads within each species were pooled and assembled using Trinity with a k-mer length of 350 bp and default parameters (v2.2.0; Grabherr et al. 2011). Second, we applied the tr2aacds analysis pipeline from EvidentialGene (http://arthropods.eugenes.org/EvidentialGene/evigene/) to identify an optimal set of transcripts, and predict the coding and amino acid sequence. We used tr2aacds pipeline to further process the transcriptome assemblies because this approach reduces the complexity of the *de novo* by filtering out of: (i) partial or fragmented transcripts; (ii) transcripts of high sequence similarity; and (iii) transcripts with low coding potential. The resulting quality of each transcriptome was determined using N50 statistics and the percentage of reads that were represented by each assembly. To do this, processed reads were mapped onto an assembly using bowtie2 (v2.2.9; Langmead et al. 2009) and percent was quantified using the Trinity utility SAM_nameSorted_to_uniq_count_stats.pl.

Quantification of gene expression for each RNA-seq library was determined using the following pipeline. First, processed reads for each species were mapped to either their respective transcriptome or genome assembly using HISAT2 with default parameters (v2.0.4; Kim et al. 2015). *Populus* data sets were mapped to the *Populus* v3.0 genome assembly (Tuskan et al. 2006) and *Eucalyptus* data sets were mapped to *Eucalyptus* v2.0 (Myburg et al. 2014). Uniquely mapped reads were counted using htseq-count (Anders et al. 2015) and expression was quantified as reads per kilobase per million reads (rpkm) using edgeR with the TMM transformation method (v3.16.5; Robinson et al. 2010).

Annotation of transcriptome and genome assemblies was performed using best *Arabidopsis* blast hit and determined from the blastp (v2.2.25; Altschul et al. 1997) results between transcript sequences and TAIR10 peptide sequences (https://www.arabidopsis.org/) with an e-value cutoff of 1e-5. Functional characterization of genes expressed in the monocot and angiosperm cambium was performed using GO terms associated with the best *Arabidopsis* blast hit. GO terms for each species were limited to expressed genes with a mean rpkm value greater than or equal to 1.0. The overlap between unique GO terms was calculated using the R package Vennerable (v3.0; https://github.com/js229/Vennerable).

Orthologous relationships between monocot transcripts and *Populus* and *Eucalyptus* gene models were

determined using inParanoid (v4.1; Remm et al. 2001; Östlund et al. 2010). Using these relationships, we investigated the evolution of gene families that have previously been described as important regulators of vascular cambium. The phylogenetic relationships between genes were generated by aligning amino acid sequences using the clustalW method using the R package msa (v1.6.0; Bodenhofer et al. 2015). The gene trees were plotted as un-rooted neighbor-joining trees using the pairwise distances of the protein alignments as implemented in the R packages ape (v4.0; Paradis et al. 2004) and seqinr (v3.3-3; Charif and Lobry 2007). The significance of branch nodes was determined using bootstrap analysis and calculated using 100 iterations.

Data availability

Sequences associated with this project are available through NCBI BioProject PRJNA374584. NCBI Short Read Archive (SRA) accessions associated with the 100 bp PE Illumina data are SRR5257973, SRR5257974, SRR5257975. The *Yucca gloriosa* transcriptome has been submitted to the NCBI Transcriptome Shotgun Assembly (TSA) database under accession GFHP00000000 and the *Cordyline australis* transcriptome to accession GFHQ00000000

ACKNOWLEDGEMENTS

We thank Courtney Canning for assistance in plant growth and cultivation. Funding for research in the Groover laboratory is from the US Forest Service, and USDA AFRI grants 2011-67013-30062 and 2014-04041. M.Z. is supported by NSF PGRP Fellowship grant IOS-1402064.

AUTHOR CONTRIBUTIONS

A.G. conceived of the study. A.G. and S.G. harvested plant tissues, performed histology, isolated RNA and prepared sequencing libraries. M.Z. performed the bioinformatics. A.G. and M.Z. interpreted the data and wrote the paper.

REFERENCES

Altschul SF, Madden TL, Schäffer AA, Zhang J, Zhang Z, Miller W, Lipman DJ (1997) Gapped BLAST and PSI-BLAST: A new generation of protein database search programs. **Nucleic Acids Res** 25: 3389–3402

Anders S, Pyl PT, Huber W (2015) HTSeq: A Python framework to work with high-throughput sequencing data. **Bioinformatics** 31: 166–169

Bodenhofer U, Bonatesta E, Horejs-Kainrath C, Hochreiter S (2015) msa: An R package for multiple sequence alignment. **Bioinformatics** 31: 3997–3999

Carlquist S (2012) Monocot xylem revisited: New information, new paradigms. **Bot Rev** 78: 87–153

Cheadle VI (1937) Secondary growth by means of a thickening ring in certain monocotyledons. **Bot Gaz** 98: 535–555

Diggle PK, DeMason DA (1983a) The relationship between the primary thickening meristem and the secondary thickening meristem in *Yucca whipplei* Torr. I. Histology of the mature vegetative stem. **Am J Bot** 70: 1195–1204

Diggle PK, DeMason DA (1983b) The relationship between the primary thickening meristem and the secondary thickening meristem in *Yucca whipplei* Torr. II. Ontogenetic relationship within the vegetative stem. **Am J Bot** 70: 1205–1216

Du J, Mansfield SD, Groover AT (2009) The *Populus* homeobox gene *ARBORKNOX2* regulates cell differentiation during secondary growth. **Plant J** 60: 1000–1014

Du J, Robischon M, Miura E, Martinez C, Groover AT (2011) The *Populus* Class III HD ZIP transcription factor *POPCORONA* affects patterning and cell differentiation during secondary growth of woody stems. **PLoS ONE** 6: e17458

Emery JF, Floyd SK, Alvarez J, Eshed Y, Hawker NP, Izhaki A, Baum SF, Bowman JL (2003) Radial patterning of *Arabidopsis* shoots by class III HD-ZIP and KANADI genes. **Curr Biol** 13: 1768–1774

Esau K (1977) *Anatomy of Seed Plants*, 2nd ed. Wiley, New York

Eshed Y, Izhaki A, Baum SF, Floyd SK, Bowman JL (2004) Asymmetric leaf development and blade expansion in *Arabidopsis* are mediated by KANADI and YABBY activities. **Development** 131: 2997–3006

Etchells JP, Mishra Laxmi S, Kumar M, Campbell L, Turner Simon R (2015) Wood formation in trees is increased by manipulating PXY-regulated cell division. **Curr Biol** 25: 1050–1055

Etchells JP, Turner SR (2010) The PXY-CLE41 receptor ligand pair defines a multifunctional pathway that controls the rate and orientation of vascular cell division. **Development** 137: 767–774

Grabherr MG, Haas BJ, Yassour M, Levin JZ, Thompson DA, Amit I, Adiconis X, Fan L, Raychowdhury R, Zeng Q, Chen Z, Mauceli E, Hacohen N, Gnirke A, Rhind N, di Palma F, Birren BW, Nusbaum C, Lindblad-Toh K, Friedman N, Regev A (2011) Full-length transcriptome assembly from RNA-Seq data without a reference genome. **Nat Biotech** 29: 644–652

Groover A, Mansfield S, DiFazio S, Dupper G, Fontana J, Millar R, Wang Y (2006) The *Populus* homeobox gene *ARBORKNOX1* reveals overlapping mechanisms regulating the

shoot apical meristem and the vascular cambium. **Plant Mol Biol** 61: 917–932

Hay A, Tsiantis M (2010) KNOX genes: Versatile regulators of plant development and diversity. **Development** 137: 3153–3165

Hirakawa Y, Kondo Y, Fukuda H (2010) TDIF peptide signaling regulates vascular stem cell proliferation via the *WOX4* homeobox gene in *Arabidopsis*. **Plant Cell** 22: 2618–2629

Ilegems M, Douet VR, Meylan-Bettex M, Uyttewaal M, Brand L, Bowman JL, Stieger PA (2010) Interplay of auxin, KANADI and Class III HD-ZIP transcription factors in vascular tissue formation. **Development** 137: 975–984

Ito Y, Nakanomyo I, Motose H, Iwamoto K, Sawa S, Dohmae N, Fukuda H (2006) Dodeca-CLE peptides as suppressors of plant stem cell differentiation. **Science** 313: 842–845

Izhaki A, Bowman JL (2007) KANADI and Class III HD-Zip gene families regulate embryo patterning and modulate auxin flow during embryogenesis in *Arabidopsis*. **Plant Cell** 19: 495–508

Joshi NA, Fass JN (2011) Sickle: A sliding-window, adaptive, quality-based trimming tool for FastQ files (Version 1.33) [Software]. Available at https://github.com/najoshi/sickle:

Jura-Morawiec J, Tulik M, Iqbal M (2015) Lateral meristems responsible for secondary growth of the monocotyledons: A survey of the state of the art. **Bot Rev** 81: 150–161

Kerstetter RA, Bollman K, Taylor RA, Bomblies K, Poethig RS (2001) KANADI regulates organ polarity in *Arabidopsis*. **Nature** 411: 706–709

Kim D, Langmead B, Salzberg SL (2015) HISAT: A fast spliced aligner with low memory requirements. **Nat Methods** 12: 357–360

Kondo Y, Fukuda H (2015) The TDIF signaling network. **Curr Opin Plant Biol** 28: 106–110

Langmead B, Trapnell C, Pop M, Salzberg SL (2009) Ultrafast and memory-efficient alignment of short DNA sequences to the human genome. **Genome Biol** 10: R25

Li E, Bhargava A, Qiang W, Friedmann MC, Forneris N, Savidge RA, Johnson LA, Mansfield SD, Ellis BE, Douglas CJ (2012) The Class II KNOX gene KNAT7 negatively regulates secondary wall formation in *Arabidopsis* and is functionally conserved in *Populus*. **New Phytol** 194: 102–115

Myburg AA, Grattapaglia D, Tuskan GA, Hellsten U, Hayes RD, Grimwood J, Jenkins J, Lindquist E, Tice H, Bauer D, Goodstein DM, Dubchak I, Poliakov A, Mizrachi E, Kullan AR, Hussey SG, Pinard D, van der Merwe K, Singh P, van Jaarsveld I, Silva-Junior OB, Togawa RC, Pappas MR, Faria DA, Sansaloni CP, Petroli CD, Yang X, Ranjan P, Tschaplinski TJ, Ye CY (2014) The genome of *Eucalyptus grandis*. **Nature** 510: 356–362

Östlund G, Schmitt T, Forslund K, Köstler T, Messina DN, Roopra S, Frings O, Sonnhammer ELL (2010) InParanoid 7: New algorithms and tools for eukaryotic orthology analysis. **Nucleic Acids Res** 38: D196–D203

Paradis E, Claude J, Strimmer K (2004) APE: Analyses of Phylogenetics and Evolution in R language. **Bioinformatics** 20: 289–290

Prigge MJ, Otsuga D, Alonso JM, Ecker JR, Drews GN, Clark SE (2005) Class III homeodomain-leucine zipper gene family members have overlapping, antagonistic, and distinct roles in *Arabidopsis* development. **Plant Cell** 17: 61–76

Remm M, Storm CE, Sonnhammer EL (2001) Automatic clustering of orthologs and in-paralogs from pairwise species comparisons. **J Mol Biol** 314: 1041–1052

Robinson MD, McCarthy DJ, Smyth GK (2010) edgeR: A Bioconductor package for differential expression analysis of digital gene expression data. **Bioinformatics** 26: 139–140

Robischon M, Du J, Miura E, Groover A (2011) The *Populus* Class III HD ZIP, *popREVOLUTA*, influences cambium initiation and patterning of woody stems. **Plant Physiol** 155: 1214–1225

Rudall P (1991) Lateral meristems and stem thickening growth in monocotyledons. **Bot Rev** 57: 150–163

Rudall P (1995) New records of secondary thickening in monocotyledons. **IAWA J** 16: 261–268

Sonnhammer ELL, Östlund G (2015) InParanoid 8: Orthology analysis between 273 proteomes, mostly eukaryotic. **Nucleic Acids Res** 43: D234–D239

Spicer R, Groover A (2010) The evolution of development of the vascular cambium and secondary growth. **New Phytol** 186: 577–592

Tomlinson PB, Zimmermann MH (1967) The "wood" of monocotyledons. **IAWA Bull** 2: 2–24

Tomlinson PB, Zimmermann MH (1969) Vascular anatomy of monocotyledons with secondary growth - An introduction. **J Arnold Arbor** 50: 159–179

Tuskan GA, Difazio S, Jansson S, Bohlmann J, Grigoriev I, Hellsten U, Putnam N, Ralph S, Rombauts S, Salamov A, Schein J, Sterck L, Aerts A, Bhalerao RR, Bhalerao RP, Blaudez D, Boerjan W, Brun A, Brunner A, Busov V, Campbell M, Carlson J, Chalot M, Chapman J, Chen GL, Cooper D, Coutinho PM, Couturier J, Covert S, Cronk Q, Cunningham R, Davis J, Degroeve S, Dejardin A, Depamphilis C, Detter J, Dirks B, Dubchak I, Duplessis S, Ehlting J, Ellis B, Gendler K, Goodstein D, Gribskov M, Grimwood J, Groover A, Gunter L, Hamberger B, Heinze B, Helariutta Y, Henrissat B, Holligan D, Holt R, Huang W, Islam-Faridi N, Jones S, Jones-Rhoades M, Jorgensen R, Joshi C, Kangasjärvi J, Karlsson J, Kelleher C, Kirkpatrick R, Kirst M, Kohler A, Kalluri U, Larimer F, Leebens-Mack J, Leple JC, Locascio P, Lou Y, Lucas S, Martin F, Montanini B, Napoli C, Nelson DR, Nelson C, Nieminen K, Nilsson O, Pereda V, Peter G, Philippe R, Pilate G, Poliakov A, Razumovskaya J, Richardson P, Rinaldi C, Ritland K, Rouze P, Ryaboy D, Schmutz J, Schrader J, Segerman B, Shin H, Siddiqui A, Sterky F, Terry A, Tsai CJ, Uberbacher E, Unneberg P, Vahala J, Wall K, Wessler S, Yang G, Yin T, Douglas C, Marra M, Sandberg G, Van de Peer Y, Rokhsar D (2006) The genome of black cottonwood, *Populus trichocarpa* (Torr. & Gray). **Science** 313: 1596–1604

Xu P, Kong Y, Song D, Huang C, Li X, Li L (2014) Conservation and functional influence of alternative splicing in wood formation of *Populus* and *Eucalyptus*. **BMC Genomics** 15: 780

Xue J, Frost C, Tsai CJ, Harding S (2016) Drought response transcriptomes are altered in poplar with reduced tonoplast sucrose transporter expression. **Sci Rep** 6: 33655

Zinkgraf M, Liu J, Groover A, Filkov V (2017) Identifying gene co-expression networks underlying the dynamic regulation of wood-forming tissues in *Populus* under diverse environmental conditions. **New Phytol** DOI:10.1111/nph.14492

SUPPORTING INFORMATION

Additional Supporting Information may be found online in the supporting information tab for this article:http://onlinelibrary.wiley.com/doi/10.1111/jipb.12538/suppinfo

Figure S1. Comparison of transcript levels for KANADI orthologs in multiple wood-forming tissues from *Populus trichocarpa* (Zinkgraf et al. 2017) and well-watered hybrid aspen (Xue et al. 2016)

Expression of all nine KANADI orthologs in *Populus* were consistently low (<1 reads per kilobase per million reads (rpkm)) in developing xylem across multiple data sets and support the lack of expression observed in Figure 6B. However, many of these orthologs displayed moderate expression in developing secondary phloem/inner bark samples from *Populus* spp. The red dashed line at 1 rpkm represents our low expression threshold.

Table S1. Tables of orthologous relationships, transcript abundance, and annotations for scaffolds and genes from the four study species

Table S2. Tables of Gene Ontology (GO) terms summarized in Venn diagram of Figure 4

Scan using WeChat with your smartphone to view JIPB online

Scan with iPhone or iPad to view JIPB online